Jurnal Teknologi

Full Paper

GRAPHENE-LAMINATED FBG FLEX SENSOR ENCAPSULATED IN SILICONE FOR HUMAN JOINT MOVEMENT MONITORING

Ibrahim Isah[a,b], Siti Mahfuza Saimon[b], Asrul Izam Azmi[b]*, Mohd Haniff Ibrahim[b], Mohd Rashidi Salim[b], Nurul Ashikin Daud[b], Muhammad Yusof Mohd Noor[b], Raja Kamarulzaman Raja Ibrahim[c]

[a]Department of Electrical Engineering, Waziri Umaru Federal Polytechnic, 860101 Birnin Kebbi, Kebbi State, Nigeria
[b]Faculty of Electrical Engineering, Universiti Teknologi Malaysia, 81310 UTM Johor Bahru, Johor, Malaysia
[c]Department of Physics, Faculty of Science, Universiti Teknologi Malaysia, 81310 UTM Johor Bahru, Johor, Malaysia

Article history
Received
28 November 2023
Received in revised form
16 December 2024
Accepted
27 January 2025
Published Online
24 October 2025

*Corresponding author
asrul@utm.my

Graphical abstract

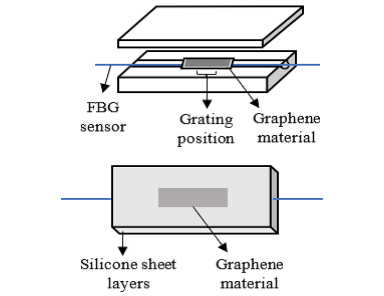

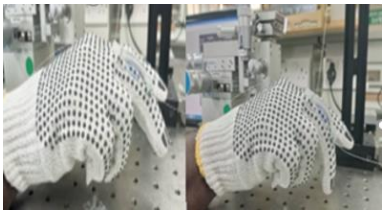

Abstract

Wearable medical devices for human joint monitoring are critical for applications such as rehabilitation, injury prevention, and performance optimization. However, capturing consistent joint motion data remains a significant challenge, requiring the development of reliable sensing technologies. This work proposes a graphene-laminated fiber Bragg grating (FBG) flex sensor encapsulated in silicone for human joint monitoring with high consistency. The sensor is formed by encapsulating an FBG and a graphene sheet between two silicone sheets, leveraging the graphene's excellent mechanical properties to enhance the interface between the silicone coating and glass fiber. Additionally, integration into hand gloves to facilitate real-time monitoring of human finger joint movements was carried out. Experimental results demonstrate that the sensor with graphene offers superior consistency across varying displacement and bending ranges. It achieved sensitivities of -0.017 nm/mm and 0.0129 nm/° for displacement and finger bending, respectively, while maintaining lower standard deviation (SD) across test cycles, indicating better performance in consistency. Conversely, the sensor without graphene exhibited higher sensitivities of -0.0199 nm/mm and 0.0258 nm/° but lacked the consistency provided by the graphene-enhanced design. The proposed sensor has huge potential in wearable medical device applications for human joint mobility measurement, particularly in musculoskeletal rehabilitation.

Keywords: Fiber Bragg grating, silicone, graphene, human joint, wavelength shift

Abstrak

Peranti perubatan boleh pakai untuk pemantauan sendi manusia adalah penting bagi aplikasi seperti pemulihan, pencegahan kecederaan dan pengoptimuman prestasi. Walau bagaimanapun, mendapatkan data gerakan sendi yang tekal kekal sebagai cabaran penting, memerlukan pembangunan teknologi penderiaan yang boleh dipercayai. Kerja ini mencadangkan penderia lenturan gentian parutan Bragg (FBG) berlamina graphene yang terkapsul dalam silikone untuk pemantauan sendi manusia dengan tahap konsistensi yang tinggi. Penderia ini dibentuk dengan melitupi FBG dan lembaran graphene di antara dua lapisan silikone, memanfaatkan sifat mekanikal graphene yang unggul untuk meningkatkan antara muka antara lapisan silikone dan gentian kaca. Selain itu, penderia ini turut disepadukan ke dalam sarung tangan untuk memudahkan pemantauan masa nyata pergerakan sendi jari manusia.

Keputusan eksperimen menunjukkan bahawa penderia dengan graphene menawarkan ketekalan unggul merentasi julat sesaran dan julat lenturan yang berbeza. Ia mencapai kepekaan -0.017 nm/mm dan 0.0129 nm/° untuk sesaran dan dan lenturan jari, sambil mengekalkan sisihan piawai (SD) yang lebih rendah merentas kitaran ujian, menunjukkan prestasi yang lebih baik dalam ketekalan. Sebaliknya, penderia tanpa graphene mempamerkan kepekaan yang lebih tinggi iaitu -0.0199 nm/mm dan 0.0258 nm/°, tetapi kurang ketekalan berbanding oleh reka bentuk yang dipertingkatkan dengan graphene. Penderia yang dicadangkan mempunyai potensi besar dalam aplikasi peranti perubatan boleh pakai untuk pengukuran pergerakan sendi manusia, terutamanya dalam pemulihan muskuloskeletal.

Kata kunci: Gentian parutan Bragg, silikone, graphene, sendi manusia, peralihan panjang gelombang

1.0 INTRODUCTION

The study of human joint mobility is critical in many medical scenarios. For instance, tasks requiring motor rehabilitation and support necessitate accurate assessment of actions carried out through ongoing joint range of motion (ROM) or movement monitoring [1, 2]. ROM is an important measurement of clinical diagnosis that helps assess joint and muscle limitations, as well as the potential risk of injury [3]. It indicates how far a joint can be flexed, extended, rotated, or otherwise moved in various directions. In order to describe changes in physical activities, the coordination of various joint movements and the changes in muscles during human body movements are identified and tracked. To some extent, this has contributed to advancements in the medical, sports, and scientific fields [4, 5].

Recently, optical fiber sensors have garnered considerable attention within the realm of rehabilitation engineering research. This surge in interest is attributable to the unique attributes of optical fibers, including their small size, high multiplexing capabilities, and inherent immunity to electromagnetic interference (EMI). These characteristics render optical fiber sensors exceptionally apt for applications involving the human body, where precision, reliability, and minimally invasive measurements are paramount. Within the category of optical fiber sensors, one notable type is fiber Bragg grating (FBG) sensors, which have a wide range of applications, including robotics, smart textiles [6, 7], plasma reactor monitoring [8], ocean engineering [9], oil and gas exploration [10], and wearable sensors [11]. In addition to these diverse applications, FBG sensors play a significant role in measuring human joint ROM and movement [12, 13]. They can be used to continuously monitor joint motions during the everyday activities of elderly individuals and post-surgery rehabilitation of various human joints like fingers, elbows, knees, or ankles. With the measurement of parameters such as angles, strain or stress, temperature, pressure, and torques, the human joint ROM can be influenced by factors such as the anatomy of the joint, surrounding muscles, ligaments, and the overall health of the individual [14].

FBG sensor can continuously monitor a patient's vital signs, providing doctors and caregivers with real-time health data. This allows for early detection of potential issues and timely interventions to prevent complications. Moreover, these technologies also enable personalized therapies, which are tailored to an individual's unique characteristics. For example, wearable sensors can be used to track a patient's movement and activity levels, which can inform the development of personalized exercise programs.

Embedding FBG sensors into protective materials such as silicone, fabric, or elastomers has shown promise for wearable applications. However, ensuring measurement consistency remains a critical challenge due to factors such as sensor placement, material properties, and environmental effects can introduce variability. For example, Li *et al*. embedded FBG sensors in silicone tubes for joint motion tracking and reported inconsistencies due to uneven strain distribution during repeated bending cycles [11]. Similarly, Ge *et al*. demonstrated that off-center embedding of FBGs in silicone sheets improved curvature sensitivity but faced challenges in achieving repeatable sensor performance due to manufacturing tolerances [15].

Material deformation is another factor that challenges the sensor's consistency. The work in [16] highlighted that the flexibility of silicone can lead to varying levels of strain transfer depending on the material's thickness, which impacts the uniformity of the FBG sensor's response over time. In another study, an FBG sensor was embedded into a 3D-printed ring to monitor the positions of body joints, specifically the elbow and knee joints. This ring was made from polylactic acid (PLA) due to its flexibility and suitability for the fused deposition modelling (FDM) fabrication method [17]. While PLA offers flexibility and compatibility with fused deposition modeling (FDM), it is not as durable or resilient under prolonged mechanical stress as other materials like silicone or elastomers. Its limited elasticity could lead to fatigue or cracking when subjected to repetitive joint movements over time. Another approach involved

embedding an FBG sensor within a special silica gel material to detect changes in strain or deformation resulting from various body postures [18]. Although silica gel provides protective support, it has a lower sensitivity to strain and temperature.

To address this challenge, this work proposes an FBG flex sensor encapsulated within two silicone sheets of distinct thicknesses to enhance its structural integrity and consistency under bending. Silicone was chosen due to its excellent flexibility, biocompatibility, and ease of integration with FBG sensors. The devised sensor structure incorporates a graphene sheet, which significantly improve measurement consistency compared to sensors without graphene. The design and operating principle of the sensor are presented in Section 2. Section 3 briefly explains the sensor development steps as well as the experimental setup for mechanical setup and real-time monitoring of finger movements. Section 4 presents the results and discussions, and finally, Section 5 offers conclusions and recommendations for future studies.

2.0 SENSOR DESIGN AND OPERATING PRINCIPLE

2.1 Principle of FBG Sensor

FBG sensor is an advanced sensor technology that has been used in many applications related to structural health monitoring. FBG sensor is a wavelength-modulated sensor, where the output wavelength is a function of strain and temperature. This relationship is described by the following equation:

$$\frac{\Delta\lambda_B}{\lambda_B} = (1-\rho_e)\Delta\varepsilon + (\alpha+\xi)\Delta T \quad (1)$$

Where $\Delta\lambda_B$ is the shift of FBG wavelength; λ_B is the initial Bragg wavelength; ρ_e is the photo-elastic coefficient, $\Delta\varepsilon$ is the mechanical strain; α is the thermal expansion coefficient; ξ is the thermo-optic coefficient; and ΔT is the change in temperature experienced by the FBG sensor. Since FBG sensors exhibit sensitivity to both mechanical strain and temperature variations, it is essential to incorporate temperature compensation in strain measurements to ensure accuracy. In our experimental setup, measurements were conducted in a controlled environment where the temperature was maintained at standard room temperature (25°C ± 1°C). This careful control of ambient temperature conditions effectively mitigated the risk of temperature-induced cross talk, thus enhancing the reliability of our strain data.

2.1 Graphene Material

Graphene is a single layer of carbon atoms arranged in a hexagonal lattice pattern. It serves as the basic building block of other carbon-based materials such as graphite, carbon nanotubes, and fullerenes. Distinguished by its remarkable mechanical properties, graphene possesses a Young's modulus of approximately 1 TPa and a tensile strength of about 130 GPa, making it one of the most rigid and robust materials known [19]. When graphene is embedded between the silicone sheets, it will follow the curvature of bending; however, it will not deform similarly to the silicone as it experiences a different amount of stress due to its high stiffness. The strong and thin characteristics of graphene will make the stress across the surface more uniformly distributed compared to silicone. These attributes of graphene significantly enhance the flex sensor's performance consistency. Due to its strong carbon-carbon bonds and atomic-scale thickness, graphene can efficiently transmit mechanical forces [20]. When a force is applied to one part of a graphene sheet, it can be transmitted across the material with minimal energy loss. This quality is pivotal in ensuring that the sensor's response to mechanical stimuli is both rapid and accurate, harnessing graphene's unique properties to optimize the sensor's functionality.

2.3 Bending Theory of a Structure

Figure 1 shows the bending model used to describe the sensor's operation. Consider a rectangular structure formed by an attachment of two silicone sheets of different thickness. An optical fiber sensor is embedded between these two layers. When the structure bends, as shown in Figure 1, the length of the structure varies along the vertical axis. At the neutral axis - the midpoint of the structure, the length remains constant regardless of whether the structure is straight or bent. Above the neutral axis, the structure is subject to compressive forces, leading to a reduction in length, while the region below the neutral axis experiences tensile forces, resulting in an extension of the structure. The strain, ε experienced at any distance, d from the neutral axis is given by [21]:

$$\varepsilon = \frac{d}{R} \quad (2)$$

Where R is the radius of the curvature due to the applied bending. This expression indicates that the strain experienced increases with greater distance from the neutral axis.

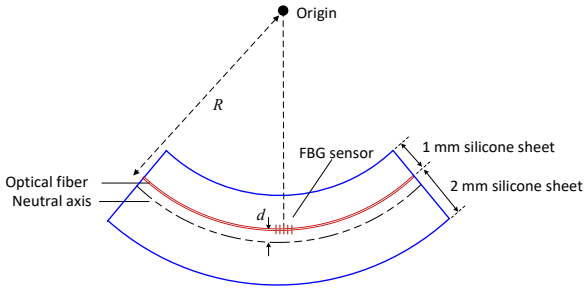

Figure 1 Bending model of the sensor structure

3.0 METHODOLOGY

3.1 Sensor Development

The FBG-based silicone sensor, designed for monitoring human joint movements, incorporates top and bottom silicone layers of varying thicknesses. The dimensions of the top and bottom layers are 50 mm × 20 mm × 1 mm and 50 mm × 20 mm × 2 mm, respectively. These dimensions were carefully selected to correspond with the anatomical structure of human joints, particularly the finger joints. A bare single-mode FBG sensor with a wavelength of 1553.9 nm was used as the sensing element and positioned inside a groove in the middle of the bottom silicone sheet. The groove was manually carved using a sharp cutter. Silicone glue was applied as an adhesive to securely bond the top and bottom silicone sheets, enclosing the optical fiber. The complete fabrication process of the sensors is depicted in Figure 2. For the devised sensor with graphene, a graphene sheet was positioned directly on the top side of FBG. All of the components were glued using silicone adhesive and was left to dry for 24 hours.

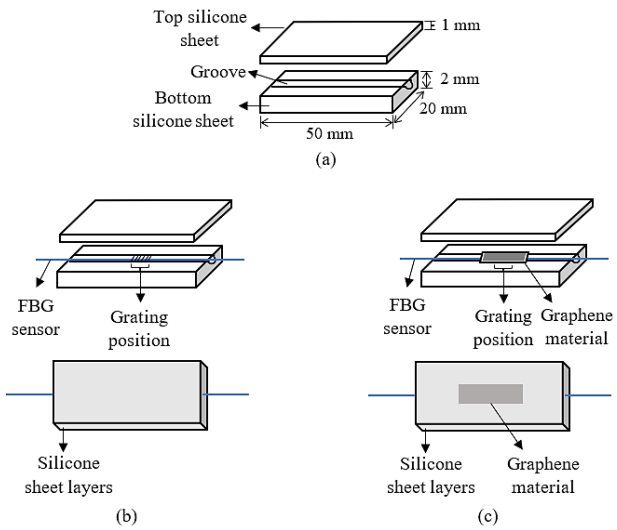

Figure 2 Development steps of the FBG sensors, (a) top and bottom silicone sheet (groove at the middle of bottom silicone sheet) (b) FBG sensor without graphene (c) FBG sensor with graphene

3.2 Experimental Setup

The experimentation with the flex sensors was conducted using a mechanical setup, as shown in Figure 3. The setup comprised a C-band amplified spontaneous emission (ASE) source that is connected to the FBG sensor and subsequently linked to an optical spectrum analyzer (OSA). FBG sensors were initially placed on a plastic ruler in a flat position (zero displacement). The plastic ruler was suspended on an adjustable metal holder on both sides. Masking tape was used to secure the sensor onto the plastic ruler to prevent shifting during displacement resulting from applied forces, which was controlled by the adjustable scale ranging from 0 mm to 28 mm. The OSA was configured with a resolution of 0.05 and sampling points of 2000. The sensor attached to the plastic ruler was displaced incrementally by 2 mm at each step, from 0 mm to 28 mm. The measurements for both sensors (with and without graphene) were repeated three times.

To facilitate real-time monitoring of human finger movements, the sensors were integrated to a hand glove. Three bending angles were examined (0°, 30°, and 60°), as illustrated in Figure 4. These angles were carefully selected to represent a range of realistic joint movements. The 0° represents the neutral position, 30° angle reflects moderate bending, which is commonly observed in everyday activities such as typing or holding objects, and finally 60° angle corresponds to significant bending such as gripping or lifting. A protractor was used to verify the angles with precision, and alignment markers were added to ensure that bending corresponded precisely to the desired angles. Similarly, the sensors (with and without graphene) underwent three repeated measurements for each bending angle.

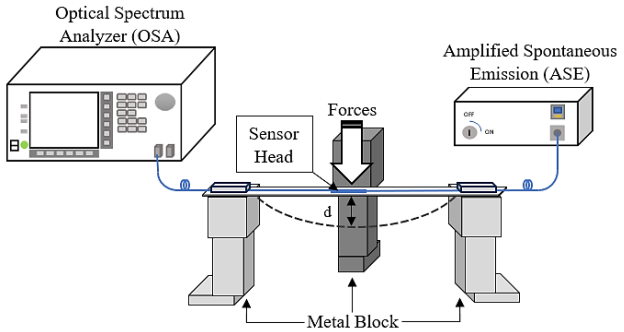

Figure 3 Mechanical setup for sensor bending measurement

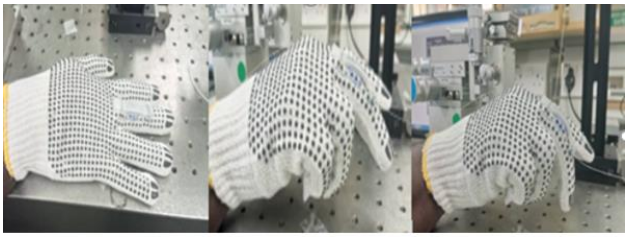

Figure 4 Real-time finger bending at angles of (a) 0°, (b) 30°, and (c) 60°

4.0 RESULTS AND DISCUSSION

Figures 5 and 6 present the transmission spectra for the displaced FBG sensor, both with and without graphene, respectively. As the displacement of the sensor increases from 0 mm to 28 mm in 2 mm increments, there is an apparent shift in the dip wavelength towards shorter wavelengths. This shift is attributed to the compression experienced by the sensor due to the applied displacement, consistent with the model described by Equation (2). The

displacement tests were repeated three times for both sensors.

Table 1 summarizes the average values and standard deviations (SD) of the FBG wavelength for both sensors across three measurement sets. Notably, the FBG sensor without graphene shows a higher SD than its graphene-enhanced counterpart from the calculated ratio. This ratio is calculated by dividing the SD of FBG without graphene with the SD of FBG with graphene. On average, the SD for the FBG sensor with graphene is approximately five times lower than that of the sensor without graphene. These results are graphically represented in Figure 7. This figure illustrates that the displacement sensitivities of the two sensors are quite comparable. Specifically, the FBG sensor without graphene exhibits a displacement sensitivity of -0.0196 nm/mm, whereas the one with graphene demonstrates a sensitivity of -0.017 nm/mm. Figure 7 clearly shows that the FBG sensor without graphene experiences its largest variation during the initial displacement, which then progressively decreases as the displacement increases.

Conversely, the FBG sensor with graphene exhibits a significantly lower SD, indicating improved repeatability. This means that the FBG with graphene reliably produces consistent strains for specific displacements. This is only possible due to the exceptional properties of graphene in transmitting mechanical force. Graphene's strong and thin characteristics ensure that stress across the surface is more uniformly distributed compared to silicone. The graphene sheet has a higher Young's modulus compared to the silicone sheet and glass optical fiber, and it will not deform under such bending force, therefore maintaining a consistent impact on the FBG and resulting in a lower SD throughout the measurements. While for the FBG without graphene, if a significant force is applied, the silicone sheet is more likely to deform before the glass because it has lower Young's modulus. This deformation leads to variability in strain transfer, as reflected by a higher SD. The use of graphene sheet has substantially improved the repeatability and reliability of the measurement.

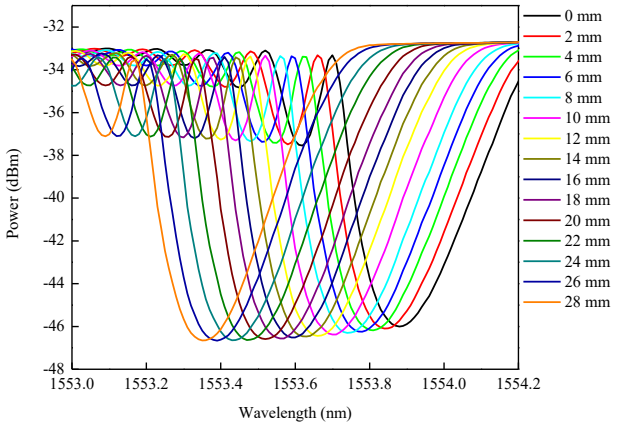

Figure 5 An example of the measured spectra at different displacement for FBG sensor with graphene

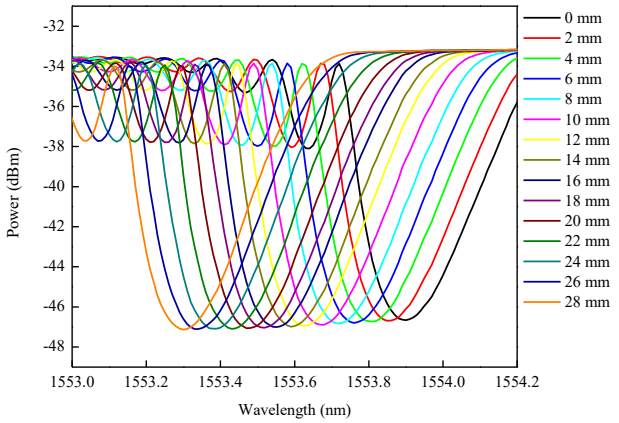

Figure 6 An example of the measured spectra at different displacement for FBG sensor without graphene

Table 1 Average and standard deviation values of the FBG wavelength, λ_B for FBG with graphene and without graphene

Disp.	Sensor with graphene		Sensor without graphene		Ratio of SD
	Ave. λ_B	SD of λ_B	Ave. λ_B	SD of λ_B	
0	1553.84	0.055	1553.84	0.149	2.71
2	1553.80	0.061	1553.79	0.143	2.35
4	1553.78	0.049	1553.75	0.134	2.72
6	1553.75	0.042	1553.71	0.123	2.95
8	1553.72	0.032	1553.67	0.108	3.36
10	1553.69	0.023	1553.63	0.100	4.34
12	1553.66	0.010	1553.60	0.087	8.74
14	1553.62	0.006	1553.56	0.079	13.75
16	1553.59	0.006	1553.52	0.076	13.11
18	1553.57	0.006	1553.48	0.072	12.53
20	1553.53	0.012	1553.44	0.061	5.27
22	1553.48	0.017	1553.40	0.058	3.33
24	1553.44	0.023	1553.35	0.044	1.89
26	1553.40	0.026	1553.30	0.040	1.53
28	1553.37	0.029	1553.84	0.026	0.92

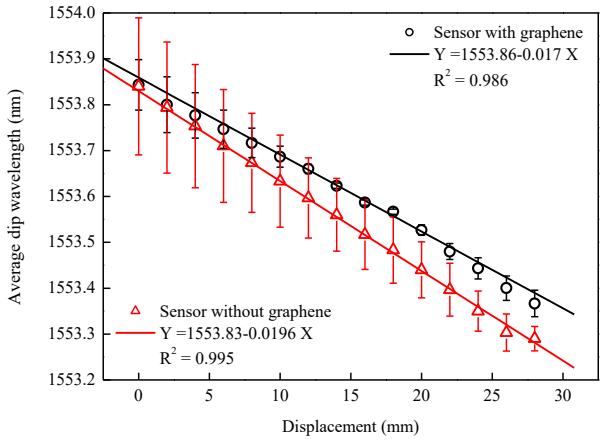

Figure 7 Average FBG wavelength with standard deviation bars versus displacement for both sensors (with and without graphene)

Both sensors were further tested on finger bending monitoring. Figure 8 shows the spectrum plots for both sensors at three bending angles, showing an increasing wavelength trend, which indicates that the sensors experienced tensile forces during finger bending. This measurement was repeated three times for each sensor. From the measurement results, the average dip wavelength and SD of both sensors were determined. For FBG without graphene, a similar issue of high wavelength variation at the initial bending procedure can be observed, as shown in Figure 8 (b). In contrast, the FBG with graphene exhibits consistent variation and relatively good linearity across three angle bending tests, as illustrated in Figure 9. The sudden transition between the first and second finger positions suggests that the FBG without graphene has the highest sensitivity during the initial finger bending from 0° to 30°. However, its consistency is quite poor due to the deformation issue. Beyond this, for bending between 30° and 60°, the FBG response shows a sign of saturation with a smaller wavelength shift.

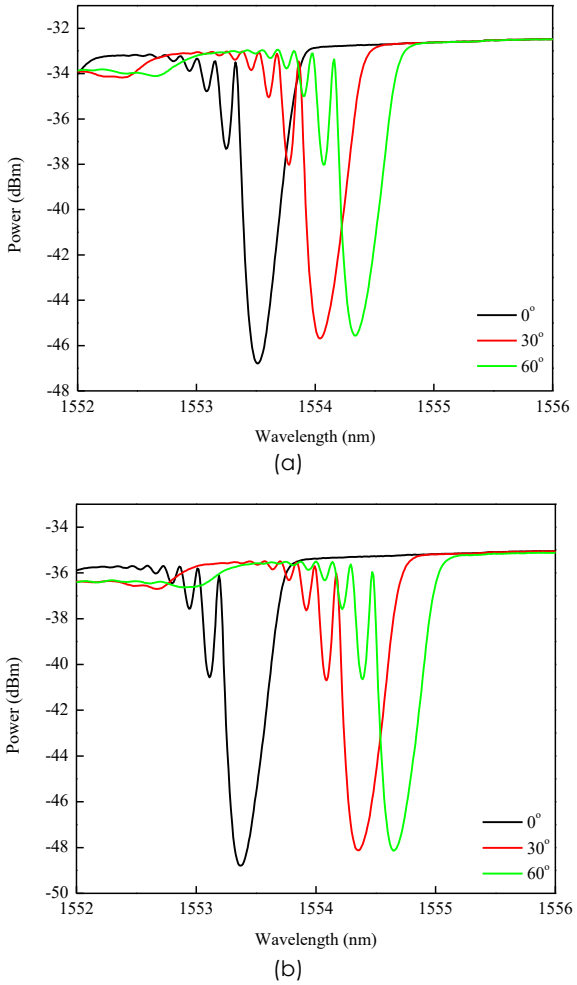

Figure 8 Spectrum waveform for real-time finger bending measurements for sensor (a) with graphene and (b) without graphene

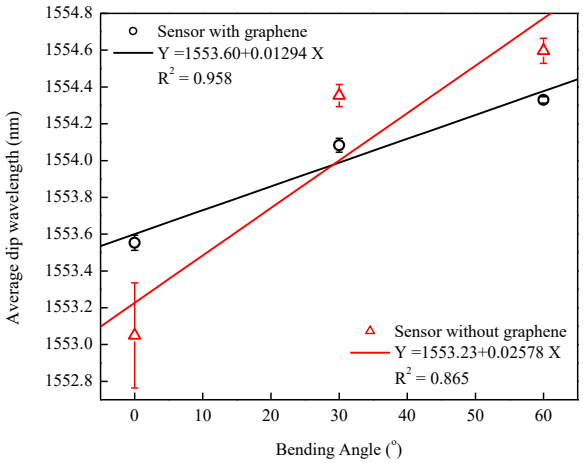

Figure 9 Average FBG wavelength with standard deviation bars versus bending angle for real-time finger bending measurements (with and without graphene FBG sensors)

5.0 CONCLUSION

This research focused on the development and evaluation of an optical flex sensor using encapsulated fiber Bragg grating (FBG) technology. The study compared the consistency and sensitivity of two FBG sensors: one with only a silicone coating and another enhanced with a silicone assisted graphene coating. The comparative analysis of sensitivity between the two sensors revealed that the FBG with graphene displayed marginally lower sensitivity than its counterpart without a graphene sheet. However, the sensor with graphene has superior performance in terms of consistency, highlights its potential for more precise and reliable measurements. Moreover, both sensors demonstrated remarkable durability during mechanical bending tests, as neither sensor sustained any damage or deterioration. This resilience underscores their suitability for long-term use in monitoring and assessing joint movements in the context of musculoskeletal rehabilitation.

Acknowledgement

The authors would like to acknowledge the financial supports from Universiti Teknologi Malaysia for the funding under UTM Fundamental Research (UTMFR) (Q.J130000.3823.23H95) and Potential Academic Staff (PAS) (Q.J130000.2723.04K07).

Conflict of Interest

The authors declare that there is no conflict of interest regarding the publication of this paper.

References

[1] Sengchuai, K., Kanjanaroat, C., Jaruenpunyasak, J., Limsakul, C., Tayati, W., Booranawong, A. and Jindapetch, N. 2022. Development of a Real-Time Knee Extension Monitoring and Rehabilitation System: Range of Motion and Surface EMG Measurement and Evaluation. *Healthcare*. 10(12): 2544. Doi: https://doi.org/10.3390/healthcare10122544.

[2] Maceira-Elvira, P., Popa, T., Schmid, A.-C. and Hummel, F. C. 2019. Wearable Technology in Stroke Rehabilitation: Towards Improved Diagnosis and Treatment of Upper-limb Motor Impairment. *Journal of NeuroEngineering and Rehabilitation*. 16(1): 142. Doi: https://doi.org/10.1186/s12984-019-0612-y.

[3] Keogh, J. W. L., Cox, A., Anderson, S., Liew, B., Olsen, A., Schram, B. and Furness, J. 2019. Reliability and Validity of Clinically Accessible Smartphone Applications to Measure Joint Range Of Motion: A Systematic Review. *PLOS ONE*. 14(5): e0215806. Doi: https://doi.org/10.1371/journal.pone.0215806.

[4] Zhou, W.-S., Lin, J.-H., Chen, S.-C. and Chien, K.-Y. 2019. Effects of Dynamic Stretching with Different Loads on Hip Joint Range of Motion in the Elderly. *Journal of Sports Science & Medicine*. 18(1): 52.

[5] Thacker, S. B., Gilchrist, J., Stroup, D. F. and Kimsey Jr, C. D. 2004. The Impact of Stretching on Sports Injury Risk: A Systematic Review of the Literature. *Medicine & Science in Sports & Exercise*. 36(3): 371–378. Doi: https://doi.org/10.1249/01.mss.0000117134.83018.f7.

[6] Issatayeva, A., Beisenova, A., Molardi, C., Tosi, D., Marques, C., Min, R., *et al*. 2019. Design of a Temperature-sensing Smart Textile based on Fiber Bragg Grating Sensor in CYTOP Fiber. *2019 SBMO/IEEE MTT-S International Microwave and Optoelectronics Conference (IMOC)*. IEEE.

[7] Li, T., Qiao, F., Huang, P., Su, Y., Wang, L., Li, X., *et al*. 2022. Flexible Optical Fiber-Based Smart Textile Sensor for Human–Machine Interaction. *IEEE Sensors Journal.* 22(20): 19336–19345. Doi: https://doi.org/10.1109/JSEN.2022.3201580.

[8] Zazwani, N., Ibrahim, R. K. R., Musa, S. M. A., Hosseinian, R., Azmi, A. I. and Ahmad, N. 2016. Reactor Temperature Profiles of Non-thermal Plasma Reactor using Fiber Bragg Grating Sensor. *Sensors and Actuators a-Physical*. 244: 206–212. Doi: https://doi.org/10.1016/j.sna.2016.04.015.

[9] Raju, Azmi, A. and Prusty, B. 2012. Acoustic Emission Techniques for Failure Characterisation in Composite Top-hat Stiffeners. *Journal of Reinforced Plastics and Composites.* 31(7): 495–516. Doi: https://doi.org/10.1177/0731684412437986.

[10] Rong, Q. and Qiao, X. 2019. FBG for Oil and Gas Exploration. *Journal of Lightwave Technology*. 37(11): 2502–2515. Doi: https://doi.org/10.1109/JLT.2018.2866326.

[11] Li, L., He, R., Soares, M. S., Savović, S., Hu, X., Marques, C., *et al*. 2021. Embedded FBG-Based Sensor for Joint Movement Monitoring. *IEEE Sensors Journal.* 21(23): 26793–26798. Doi: https://doi.org/10.1109/JSEN.2021.3120995.

[12] Jha, C. K., Gajapure, K. and Chakraborty, A. L. 2021. Design and Evaluation of an FBG Sensor-Based Glove to Simultaneously Monitor Flexure of Ten Finger Joints. *IEEE Sensors Journal*. 21(6): 7620–7630. Doi: https://doi.org/10.1109/JSEN.2020.3046521.

[13] Hu, X., Xu, Y., Zhang, H., Xie, J., Niu, D., Zhao, Z. and Qu, X. 2023. The Fiber Bragg Grating (FBG) Sensing Glove: A Review. *IEEE Sensors Journal.* 23(11): 11374–11382. Doi: https://doi.org/10.1109/JSEN.2023.3266766.

[14] Liu, C.-L., Zhou, J.-P., Sun, P.-T., Chen, B.-Z., Zhang, J., Tang, C.-Z. and Zhang, Z.-J. 2020. Influence of Different Knee and Ankle Ranges of Motion on the Elasticity of Triceps Surae Muscles, Achilles Tendon, and Plantar Fascia. *Scientific Reports.* 10(1): 6643. Doi: https://doi.org/10.1038/s41598-020-63730-0.

[15] Ge, J., James, A. E., Xu, L., Chen, Y., Kwok, K. W. and Fok, M. P. 2016. Bidirectional Soft Silicone Curvature Sensor Based on Off-Centered Embedded Fiber Bragg Grating. *IEEE Photonics Technology Letters.* 28(20): 2237–2240. Doi: https://doi.org/10.1109/LPT.2016.2590984.

[16] Di Palma, P., De Vita, E., Iadicicco, A. and Campopiano, S. 2023. Force Sensor Based on FBG Embedded in Silicone Rubber. *IEEE Sensors Journal.* 23: 1172–1178. Doi: https://doi.org/10.1109/JSEN.2022.3226039.

[17] Cheng-Yu, H., Ahmed Abro, Z., Yi-Fan, Z. and Ahmed Lakho, R. 2021. An FBG-based Smart Wearable Ring Fabricated using FDM for Monitoring Body Joint Motion. *Journal of Industrial Textiles.* 50(10): 1660–1673. Doi: https://doi.org/10.1177/1528083719870204.

[18] Abro, Z. A., Zhang, Y.-F., Hong, C.-Y., Lakho, R. A. and Chen, N.-L. 2018. Development of a Smart Garment for Monitoring Body Postures based on FBG and Flex Sensing Technologies. *Sensors and Actuators A: Physical.* 272: 153–160. Doi: https://doi.org/10.1016/j.sna.2018.01.052.

[19] Sakhaee-Pour, A. 2009. Elastic Properties of Single-layered Graphene Sheet. *Solid State Communications.* 149(1–2): 91–95. Doi: https://doi.org/10.1016/j.ssc.2008.09.050.

[20] Guo, X., Zhang, Y., An, J., Zhang, Q., Wang, R. and Yu, X. 2023. Experimental Investigation on Characteristics of Graphene Acoustic Transducers Driven by Electrostatic and Electromagnetic Forces. *Ultrasonics.* 127. Doi: https://doi.org/10.1016/j.ultras.2022.106857.

[21] Ferdinand P. Beer, E. Russell Johnston Jr., John T. DeWolf and David F. Mazurek. 2015. *Mechanics of Materials* (7th Edition). New York: McGraw Hill.